Proceedings of Asia International Conference on Tribology 2018, pp. 3-5, September 2018

Erosion wear resistance of laser cladding $AlCr_2FeCoNiNb_x$ high-entropy alloy coatings

X.L. Ji[1,2,*], Y.Y. Bao[1], J.H. Zhao[1], P. Gu[1]

[1)] College of Mechanical & Electrical Engineering, Hohai University, Changzhou 213022, China.
[2)] Engineering Research Center of Dredging Technology of Ministry of Education, Hohai University, Changzhou 213022, China.

[*]Corresponding e-mail: xiulinji@gmail.com

Keywords: Laser cladding; high-entropy alloy; erosion resistance

ABSTRACT –$AlCr_2FeCoNiNb_x$ (x=0, 0.5, 1.0, 1.5, 2.0, x values in molar ratio) high-entropy alloy (HEA) coatings were fabricated on Q345 steel by laser cladding. The effects of annealing on microstructure and erosion wear resistance of the HEA coatings were studied. These HEA coatings present an erosion characteristic of ductile materials. With addition of Nb, the Vickers hardness of $AlCr_2FeCoNiNb_x$ coatings increases due to the increase of volume fraction of Laves phase. Meanwhile, the mass loss rates decreased with the increase of Nb content. The erosion mechanism evolved from delamination to micro-ploughing with the Nb additions at 30° impact angle.

1. INTRODUCTION

High-entropy alloy (HEA) has been reported to display many outstanding properties, such as high hardness, excellent wear resistance and corrosion resistance (Zhang et al., 2014) (Miracle & Senkov, 2017). HEA coatings were fabricated by laser cladding recently (Joseph et al., 2015), showing it has excellent performance although this technology is still in its infancy. In this paper, the $AlCr_2FeCoNiNb_x$ (x=0.0, 0.5, 1.0, 1.5, 2.0, x values in molar ratio) HEAs were prepared by laser cladding. Effect of Nb addition and annealing on the microstructure and properties of the HEA coatings were investigated in detail.

2. EXPERIMENTAL PROCEDURES

Q345 steel was used as the substrate material and using a grinder to remove surface dirt. The purities of each alloy powder (Al, Fe, Cr, Ni, Co and Nb) were higher than 99.5 wt% and mixing the powder into the ball mill for 15 hours. The composition of $AlCr_2FeCoNiNb_x$ (x=0.0, 0.5, 1.0, 1.5, 2.0, x values in molar ratio). Then mixed thoroughly with the PVC solvent (4.5 wt%), pre-coated uniformly on the surface of the substrate (the layer thickness is about 0.8 mm) and baked in a drying oven for three hours. Laser cladding was carried out by pulsed laser processing machine (GD-ECYW300). The samples were cut into pieces of 10 ×10 ×10 mm by wire cutting for heating treatment and erosion experiments. The samples were heated, at a heating rate of 10℃ /min, and kept at the 650℃ for 2 h, then taken out of furnace. During all of the annealing, argon flow was used as a protective atmosphere room temperature and open to the air.

The erosion test was carried out on a slurry erosion test rig. Angular quartz particles (about HV 1100) with the mean size of 350-780μm were obtained from Yangtze Delta. For each erosion test, the slurry pot was filled with 1 cm^3 aqueous solution containing 1 wt% sand particles. All the samples were firstly polished by SiC paper in a grit of #800 and degreased in acetone, then cleaned by alcohol and air-dried. All the specimens were ultrasonically cleaned in acetone before and after each test and weighted for the total mass loss using a precision electronic balance with a sensitivity of 0.1 mg.

3. RESULTS AND DISCUSSION

XRD patterns of $AlCr_2FeCoNiNb_x$ (x=0, 0.5, 1.0, 1.5 and 2.0, denoted as Nb0, Nb0.5, Nb1.0, Nb1.5 and Nb2.0, respectively) high-entropy alloy coatings as cladding are shown in Fig. 1. The pattern of Nb0 shows a single FCC solid solution phase. Adding Nb into the Nb0 alloy coating results in the formation of BCC and Laves phase. The Laves phase was identified as the $(Co, Fe)_2(Cr, Nb)$. With the increment of the Nb content, the relative intensity of the FCC diffraction peak is reduced and almost disappear when x≥1.0, while BCC and Laves phase diffraction peaks enhance gradually after x≥0.5, indicating that the addition of Nb elements changes the phase distribution within the coating.

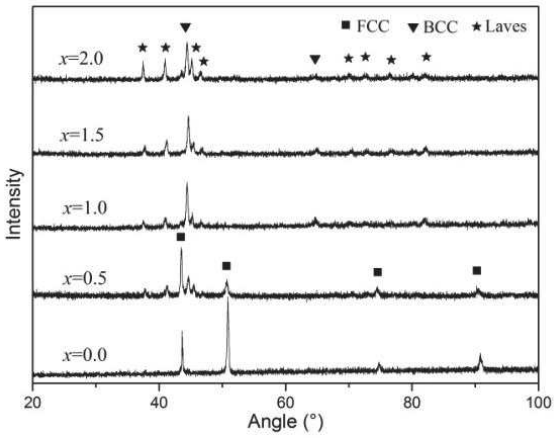

Figure 1 XRD patterns of $AlCr_2FeCoNiNb_x$ HEA coatings as cladding.

Microstructures of as-cladding and annealed HEA coatings are displayed in Fig. 2 and Fig. 3. Compared with the cladding layer, morphology of Nb0.5 and Nb1.0 changed greatly and each phase interinfiltrates each other, while the equiaxed crystal and dendrite in the microstructure of Nb0, Nb1.5 and Nb2.0 grew, as shown in Fig. 3. In alloy Nb0.5, the volume fraction of

the BCC phase decreases, both FCC and Laves phases are well-distributed relatively. The main phase is still the BCC and Laves phase corresponding to the DR region, while a small amount of the FCC phasenucleates and grows in Nb1.0. After the heat treatment, the Nb content in the FCC phase increased obviously, indicating that the annealing treatment changed the distribution of elements between the phases, resulting in the change of the microstructure in the coating.

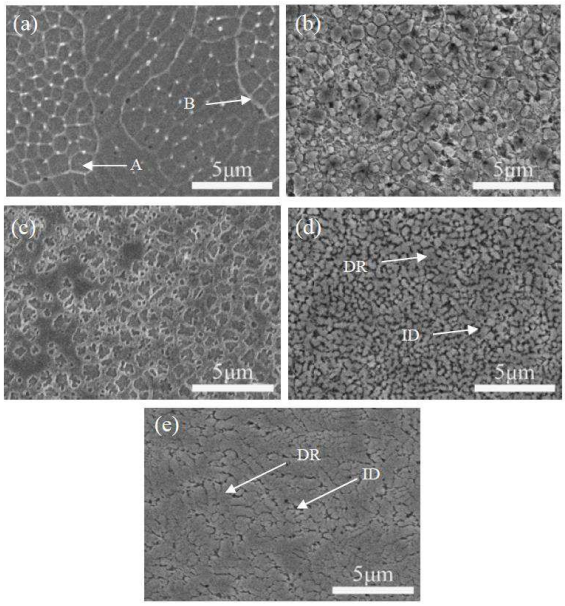

Figure 2 SEM images of as-cladding $AlCr_2FeCoNiNb_x$ HEA coatings, x=0, x=0.5, x=1.0, x=1.5 and x=2.0 corresponding to (a), (b), (c), (d) and (e).

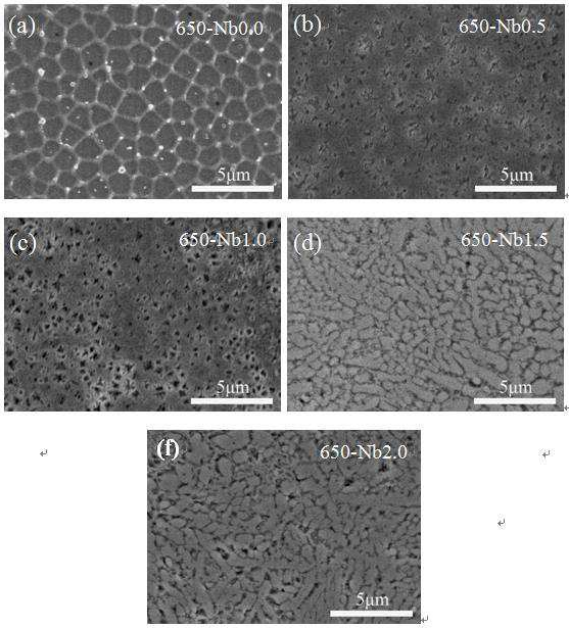

Figure 3 SEM images of annealed $AlCr_2FeCoNiNb_x$ HEA coatings, x=0, x=0.5, x=1.0, x=1.5 and x=2.0 corresponding to (a), (b), (c), (d) and (e).

The hardness of Nb0.5, Nb1.0, Nb1.5 and Nb2.0 is higher than that of Nb0.0 and the value increases with the Nb addition, as shown in Fig. 4. The maximum value is about HV 820, indicating that the increase of Nb plays a positive role in the hardness of coating.

The mass loss rates of coatings decreased with the increase of Nb content, as shown in Fig. 5. And the mass loss under 90° impingement angle is lower than that 30°. It suggests that the increase of Nb content improves the erosion resistance of the coatings and $AlCr_2FeCoNiNb_x$ high-entropy alloy coatings show the characteristics similar to those of ductile materials.

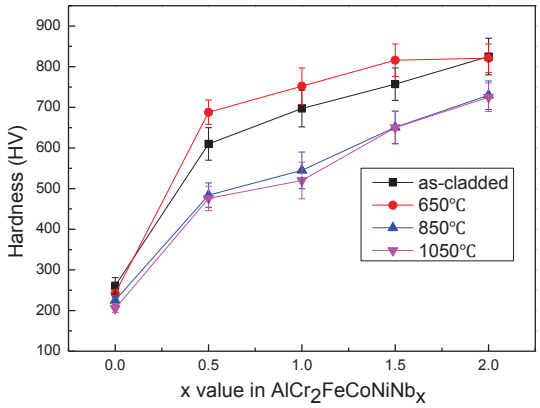

Figure 4 Vickers hardness values of $AlCr_2FeCoNiNb_x$ (x=0, 0.5, 1.0, 1.5, 2.0) HEA coatings before and after annealing.

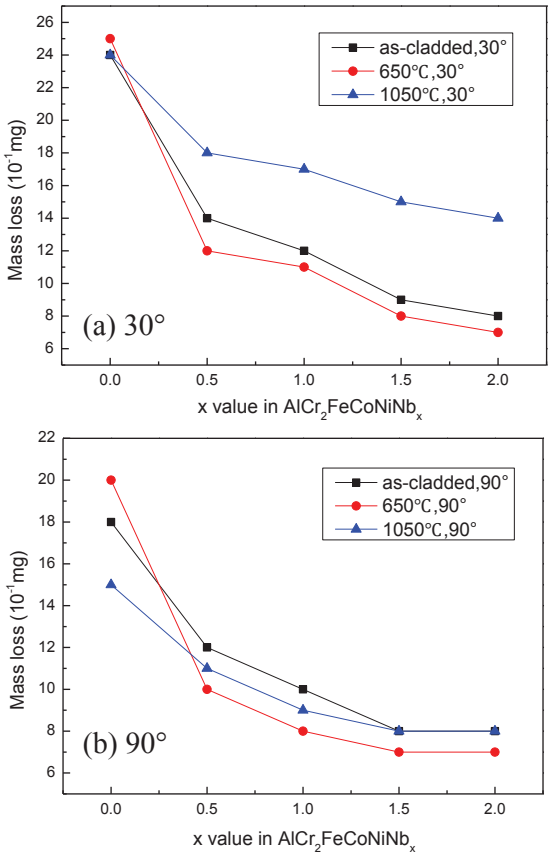

Fig. 5 Mass loss of as-cladding $AlCr_2FeCoNiNb_x$ HEA coatings as a function of x value at 30° (a) and 90° (b) impingement angle.

After adding the Nb element, the main phase changed from the soft FCC to the hard-eutectic structure (BCC+Laves) with the increase of Nb content, smoother worn surfaces can be observed in Fig. 6(b-e) and the main wear mechanism are predominant by micro-ploughing. The main feature of the worn surfaces of the surface is a lot of long traces of plowing. In conclusion, the addition of Nb is beneficial to improve the erosion resistance of the coating, which can be attributed to BCC and Laves phase.

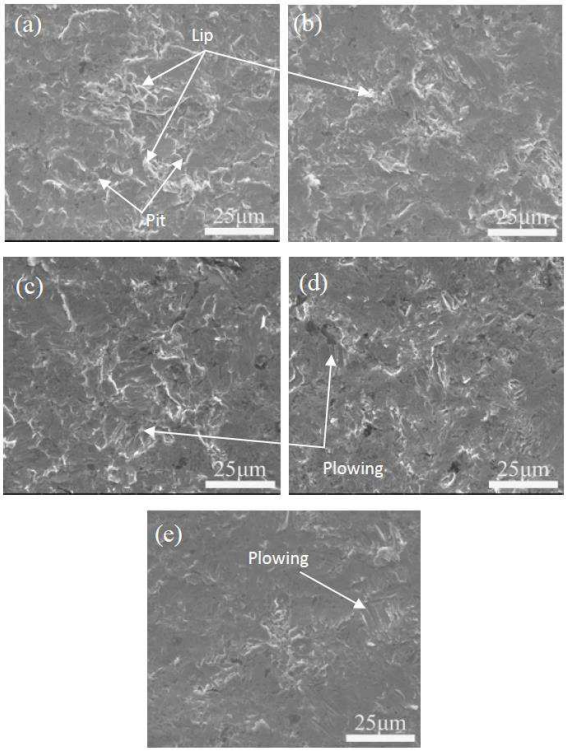

Figure 6 Eroded surface morphologies of $AlCr_2FeCoNiNb_x$ HEA coatings (as-cladding) after erosion, x=0, x=0.5, x=1.0, x=1.5, x=2.0 corresponding to (a), (b), (c), (d) and (e).

4. SUMMARY

$AlCr_2FeCoNiNb_x$ (x=0, 0.5, 1.0, 1.5, 2.0, x values in molar ratio) high-entropy alloy (HEA) coatings were fabricated on Q345 steel by laser cladding. With the addition of Nb content, the Vickers hardness of $AlCr_2FeCoNiNb_x$ coatings increases gradually before and after annealed due to the increase of volume fraction of Laves phase. The mass loss rates of coatings decreased with the increase of Nb content.

REFERENCES

[1] Joseph, J., Jarvis, T., Wu, X. H., Stanford, N., Hodgson, P., & Fabijanic, D. M. (2015). Comparative study of the microstructures and mechanical properties of direct laser fabricated and arc-melted AlxCoCrFeNi high entropy alloys. *Materials Science And Engineering a-Structural Materials Properties Microstructure And Processing*, *633*, 184-193.

[2] Miracle, D. B., & Senkov, O. N. (2017). A critical review of high entropy alloys and related concepts. *Acta Materialia, 122*(Supplement C), 448-511. doi: https://doi.org/10.1016/j.actamat.2016.08.081

[3] Zhang, Y., Zuo, T. T., Tang, Z., Gao, M. C., Dahmen, K. A., Liaw, P. K., & Lu, Z. P. (2014). Microstructures and properties of high-entropy alloys. *Progress in Materials Science, 61*, 1-93.